POLITECNICO DI TORINO
Repository ISTITUZIONALE

A Smart Measuring System for Vehicle Dynamics Testing

Original
A Smart Measuring System for Vehicle Dynamics Testing / Galvagno, E., Mauro, S., Pastorelli, S., Servetti, A., Tota, A.. - In: SAE TECHNICAL PAPER. - ISSN 0148-7191. - STAMPA. - 1:(2020), pp. 1-11. (SAE 2020 World Congress Experience, WCX 2020 Detroit, MI, USA 21-23 Aprile 2020) [10.4271/2020-01-1066].

Availability:
This version is available at: 11583/2837497 since: 2020-06-26T22:30:43Z

Publisher:
SAE International

Published
DOI:10.4271/2020-01-1066

Terms of use:

This article is made available under terms and conditions as specified in the corresponding bibliographic description in the repository

Publisher copyright
GENERICO -- per es. Nature : semplice rinvio dal preprint/submitted, o postprint/AAM [ex default]

The original publication is available at https://doi.org/10.4271/2020-01-1066 / http://dx.doi.org/10.4271/2020-01-1066.

(Article begins on next page)

09 October 2026

2020-01-1066

A Smart Measuring System for Vehicle Dynamics Testing

Author, co-author (Do NOT enter this information. It will be pulled from participant tab in MyTechZone)

Affiliation (Do NOT enter this information. It will be pulled from participant tab in MyTechZone)

Abstract

A fast measurement of the car handling performance is highly desirable to easily compare and assess different car setup, e.g. tires size and supplier, suspension settings, etc. Instead of the expensive professional equipment normally used by car manufacturers for vehicle testing, the authors propose a low-cost solution that is nevertheless accurate enough for comparative evaluations. The paper presents a novel measuring system for vehicle dynamics analysis, which is based uniquely on the sensors embedded in a smartphone and therefore completely independent on the signals available through vehicle CAN bus. Data from tri-axial accelerometer, gyroscope, GPS and camera are jointly used to compute the typical quantities analyzed in vehicle dynamics applications. In addition to signals such as yaw rate, lateral and longitudinal acceleration, vehicle speed and trajectory, normally available when working with Inertial Measurement Units (IMU) equipped with GPS, in the presented application the steering wheel angle is also measured, without additional sensors. The latter signal, besides being important for identifying the maneuver imposed by the driver, enables the usage of Kalman filters based on dynamic vehicle models (e.g. the single-track model) for the estimation of body sideslip angle. The system was tested during experimental campaigns on test tracks and the comparison between data from a professional measuring equipment and the Smart Measuring System showed a very good match. In the paper, hardware installation of smartphone and related accessories is discussed together with the main tasks of the algorithm implemented in the application, i.e. identification of smartphone orientation, steering wheel angle measurement, Kalman filter sideslip angle estimators (based on kinematic and single-track models). Furthermore, the time histories of the vehicle dynamics quantities during a lap on a handling test track are shown and compared with reference signals from the professional equipment. The proposed system proved to be a promising cost- and time-effective solution for vehicle dynamics testing.

Introduction

The adoption of measuring systems in automotive filed is essential for vehicle dynamics analysis and control system design [1,2]. For a complete description of vehicle motion, a set of signals needs to be recorded and monitored when experimental maneuvers are executed [3,4]. This set of quantities may include vehicle body kinematics, i.e. global vehicle position together with its linear and angular speeds and accelerations, tires kinematics and dynamics, i.e. wheel rotational speeds and tires-terrain contact forces, as well as driver-imposed input, such as steering wheel angle, gas and brake pedal positions and engaged gear.

A basic approach consists of monitoring all the desired quantities through direct sensor measurements; accelerations are commonly measured by tri-axial accelerometers, angular speeds by gyroscopes and global position by GPS antenna. All these quantities are usually measured by professional IMU which includes the measurements set into a unique compact sensor. The direct measurement represents, in some cases, the most expensive solution since some quantities, such as vehicle speed components, usually require extremely expensive equipment which may include optical sensors [5] or high precision differential GPS [6-10] that relies on real time corrections coming from fixed-sight antenna (i.e. RTK corrections). A second approach may involve the vehicle network system. Driver input, for instance, are usually extracted from the vehicle CAN network. A larger set of data can be read from the CAN network, including vehicle longitudinal speed estimated from wheels angular speed. Unfortunately, the CAN communication is not available for common vehicle users. The last solution involves the implementation of estimators [11,12]: most of the professional data acquisition systems adopt Kalman Filters algorithms to estimate non-measurable quantities, such as lateral speed components, sideslip angle, roll and pitch angles, or to improve the robustness of available measurements. The Kalman Filter always relies on vehicle dynamics models which may include kinematic relations [13,14], dynamic equations [15-17], or a combination of both solutions [18]. Most of the time, a combination of the three solutions represents a good compromise among economic constraints, available onboard space for instrumentation installation and accessibility to vehicle CAN network.

Differently from other low-cost solutions [19,20], the present paper describes a Smart Measuring System able to satisfy the following characteristics:

- Provide vehicle center of gravity accelerations, velocities and global position, angular velocities, steering wheel angle and sideslip angle
- To be independent from vehicle CAN network
- Require an easy and noninvasive installation and calibration
- To be based on low-cost ($\leq$ 1000 €) and widely available components

The Smart Measuring System aims to be an attractive solution for both amateur and professional users who just need a ready-to-use acquisition system for preliminary experimental evaluation. It consists of an APP that processes off-line the data measured from sensors conventionally embedded on a smartphone. The APP also adopts the rear-facing camera of the smartphone to evaluate the steering wheel angle applied by the driver, which represents a more transparent and non-invasive solution with respect to other ones [21-23]. The steering

wheel angle information is also used as input for two cascade Kalman Filters which are implemented to estimate the sideslip angle.

The paper is divided into the following sections: the first one introduces the smart measuring system together with a professional data acquisition system used as reference for test validation; the second section is related to the main tasks of the smartphone application, i.e. identification of smartphone orientation, steering wheel angle measurement and sideslip angle estimation; experimental signals comparison from the two data acquisition systems are then shown in the next section. Finally, the outlines of the research are listed in the conclusions.

Data acquisition systems

For the purpose of validating the smart measuring system, a professional data acquisition system by REMAK is adopted which includes the following components:

- A VBOX 3i Dual Antenna (VB3iSL) with a GPS/GLONASS receiver to achieve high level accuracy of global position and vehicle speed
- Racelogic's Inertial Measurement Unit (RLVBIMU04-V2) provides highly accurate measurements of pitch, roll, and yaw rate using three rate gyros, as well as x, y, z acceleration via three accelerometers

The REMAK data acquisition system is also enhanced by the presence of Kalman Filter algorithm to estimate roll, pitch and sideslip angles and to depurate the vehicle accelerations from roll and pitch motions.

The Smart Measuring System relies on the set of sensors commonly available on nowadays smartphones. In this application, the smartphone sensors set includes the following components:

- LSM6Dl 6-axis inertial sensor representing a system-in-package featuring a MEMS 3D digital accelerometer and a 3D digital gyroscope for low-power consumption accelerations and angular speeds measurements
- GPS/GLONASS/BeiDou/Galileo single antenna receiver for global position measurement
- SM-G950W 12 MP rear-facing camera module with a IMX333 Sony sensor, used for recording the steering wheel angle motion

Smartphone application tasks

The algorithm here presented receives and processes the smartphone raw data in order to provide a direct measurements of vehicle accelerations, angular speeds and global position enhanced by an estimation of steering wheel angle, sideslip angle and longitudinal speed.

A general scheme of the algorithm is represented in Fig. 1 by showing three main steps:

1. Coordinate reference system transformation from the smartphone-based system to the vehicle-based one
2. Estimation of steering wheel angle from smartphone camera video frames
3. Estimation of sideslip angle

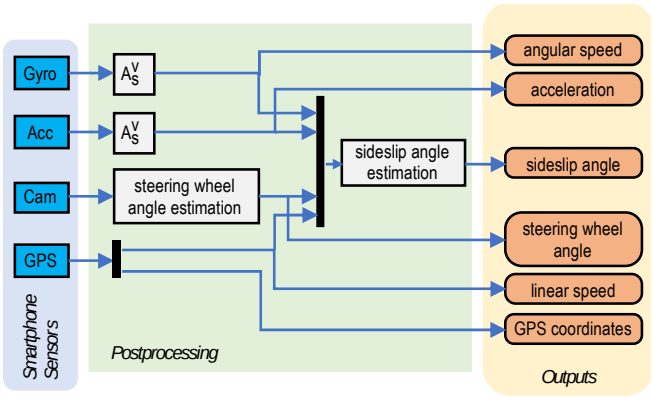

Figure 1. General scheme of the algorithm implemented by the Smart Measuring System.

The application developed is designed to calibrate the Smart Measuring System, to measure and save smartphone sensors raw data, to run the algorithm off-line at the end of the maneuver thus finally plotting the desired quantities on the smartphone display.

Identification of smartphone orientation

The measurement of vehicle dynamics quantities requires the definition of specific coordinate reference systems. Three reference frames are thus considered, as shown in Fig.2:

- Ground absolute reference frame R_O (X_O, Y_O, Z_O axes) adopted to express the global vehicle position and orientation
- Vehicle reference frame R_V (X_V, Y_V, Z_V axes) located in the vehicle center of gravity and oriented according the to vehicle longitudinal and lateral axes; it is a non-inertial reference frame since it moves together with the vehicle but it does not roll or pitch, thus allowing the definition of vehicle roll and pitch angles
- Smartphone reference system R_S (X_S, Y_S, Z_S axes) which position and orientation depends on the specific installation of the smartphone inside the vehicle; it is a non-inertial reference frame since it moves and rotates according to the vehicle sprung mass

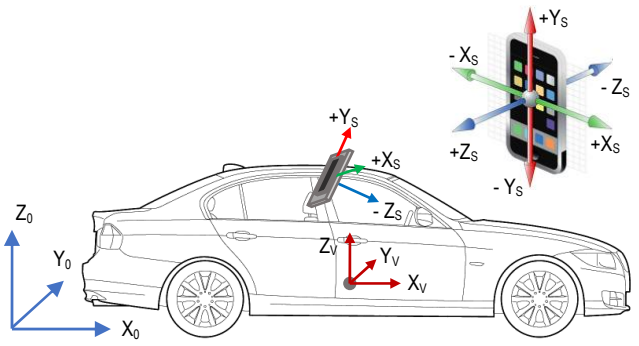

Figure 2. Coordinate reference systems definition: 0 (ground), V (vehicle), S (smartphone) reference frames.

The smartphone can be placed in a specific position by means of a suction holder in order to point the steering wheel angle with its rear

facing camera. Generally, the smartphone reference frame does not coincide with the vehicle one, where most of the quantities are tipically analyzed, including linear accelerations and angular speeds.

A suitable rotation matrix is then used to transform vector quantities, originally measured in the smartphone reference frame, to vectors expressed with respect to the vehicle reference frame, according the following equation:

$$r_V = A_S^V \, r_S \qquad (1)$$

where A_S^V is the rotation matrix containing the direction cosines defining the orientation of the smartphone reference frame with respect to the vehicle frame; r_S and r_V are the set of components of a generic vector quantity r expressed with respect to frames R_S and R_V respectively.

A calibration procedure is therefore designed to automatically get the rotation matrix A_S^V when the Smart Measurement System is installed. It is based on acceleration measures during specific maneuvers the driver is requested to perform:

1. **Stationary vehicle**: since the gravity is the only acceleration measured by the system in this condition, this phase is used to detects the Z_V axis
2. **Acceleration and deceleration of the vehicle on a straight line**: since the vehicle has null lateral acceleration in this condition, this phase is used to detects the $< X_V, Z_V >$ plane

By executing the two calibration phases, since the vehicle lateral and vertical acceleration components are constantly null or equal to the gravity respectively, the measured acceleration vectors are expected to lie on the plane identified by the Z_V and X_V axes. At the same time, since the smartphone is rotated with respect to the vehicle frame, the measured acceleration vectors lie on a plane that is expected to be rotated as well with respect to the smartphone frame. An example of the acceleration data measured by the smartphone during the calibration procedure is shown in Fig.3. In the figure, the points cloud represents the tips of the acceleration vectors with tails at the origin of the graph axes.

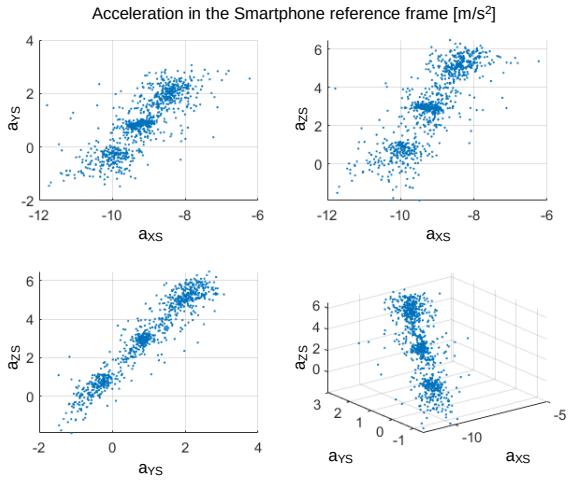

Figure 3. Acceleration components of the vehicle measured by the smartphone, in the smartphone reference frame, during calibration.

A fitting plane is calculated as the plane passing through the origin of the smartphone frame and the points cloud. The axis perpendicular to the fitting plane is the Y_V axis. Assuming that the direction of Z_V axis is identified by the data with stationary vehicle, the X_V axis is evaluated to complete a right-handed frame together with Y_V and Z_V axes. The resulting orientation of the smartphone frame with respect to the vehicle frame of the data represented in Fig. 3 is shown in Fig. 4. As a matter of facts, the points cloud has a main axis parallel to the vehicle longitudinal X_V axis, the rear face of the smartphone (identified by the $-Z_S$ axis) points frontward, and the longitudinal Y_S axis of the smartphone is approximately parallel to the vehicle lateral Y_V axis; that means an approximately horizontal holding positioning of the smartphone.

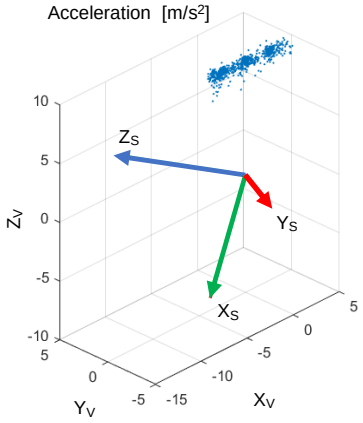

Figure 4. Smartphone reference frame with respect to the vehicle reference frame resulting from the calibration procedure.

The orientation matrix evaluated during the Smart Measuring System calibration is then applied to transform the gyroscope and the accelerometer data from the smartphone reference frame to the vehicle reference frame according to Eq. 1.

Moreover, the vehicle center of gravity acceleration has to be evaluated for vehicle dynamics estimation. The acceleration components of the vehicle center of gravity are calculated from the angular speed and angular acceleration, since they represent a property of the sprung mass and do not depend on the measurement point:

$$\begin{bmatrix} a_{x_S} \\ a_{y_S} \\ a_{z_S} \end{bmatrix} = \begin{bmatrix} a_{x_G} \\ a_{y_G} \\ a_{z_G} \end{bmatrix} + \begin{bmatrix} \ddot{\varphi}\, z_S - (\dot{\varphi}^2 + \dot{\psi}^2)\, x_S - \ddot{\psi}\, y_S + \dot{\psi}\, \dot{\theta}\, z_S + \dot{\varphi}\, \dot{\theta}\, y_S \\ \ddot{\psi}\, x_S - (\dot{\theta}^2 + \dot{\psi}^2)\, y_S - \ddot{\theta}\, z_S + \dot{\psi}\, \dot{\varphi}\, z_S + \dot{\varphi}\, \dot{\theta}\, x_S \\ \ddot{\theta}\, y_S - (\dot{\theta}^2 + \dot{\varphi}^2)\, z_S - \ddot{\varphi}\, y_S + \dot{\theta}\, \dot{\psi}\, x_S + \dot{\varphi}\, \dot{\psi}\, y_S \end{bmatrix} \qquad (2)$$

where $[a_{x_S}\ a_{y_S}\ a_{z_S}]^t$ and $[a_{x_G}\ a_{y_G}\ a_{z_G}]^t$ are the smartphone and vehicle center of gravity acceleration components, both expressed in the vehicle reference frame, $\dot{\psi}$ and $\ddot{\psi}$ are the yaw rate and yaw acceleration, $\dot{\theta}$ and $\ddot{\theta}$ are the roll rate and roll acceleration, $\dot{\varphi}$ and $\ddot{\varphi}$ are the pitch rate and pitch acceleration and $[x_S\ y_S\ z_S]$ is the vector of the smartphone position with respect to the vehicle reference frame centered in its center of gravity.

It is important to underline that Eq. 2 is not always applicable since the position of the vehicle center of gravity is not always a known

parameter and $\ddot{\psi}$, $\ddot{\theta}$, $\ddot{\varphi}$ are not directly measured by the smartphone sensors. Evaluation of the angular acceleration should require an estimation algorithm applied to the angular speed, nevertheless, if the smartphone is placed on the driver or front passenger window, it can be reasonably supposed that it is sufficiently close to the vehicle center of gravity, thus neglecting the distances x_S, y_S and z_S.

Steering wheel angle measurement

The steering wheel angle represents one of the most important information for correlating all vehicle dynamics quantities to driver input and to allow the estimation of non-measurable quantities such as the sideslip angle. The Smart Measuring System adopts the rear-facing camera to record the position of ArUco makers set, previously placed on the steering wheel angle. An algorithm based on the Computer Vision Matlab toolbox is then used for detecting the markers positions at different time instants thus providing an estimation of the relative steering wheel angle imposed by the driver with respect to the zero-position detected during the calibration phase. This methodology is promising since it not invasive, does not require the communication with the vehicle CAN network and it does not require that the camera is perfectly placed in front of the steering wheel.

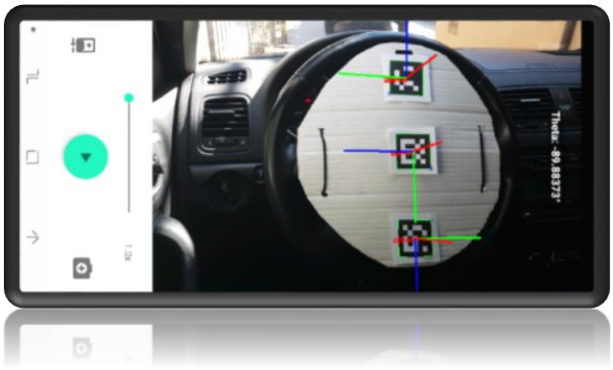

Figure 5. Markers detection through the rear-facing camera.

The markers are usually installed on a white plate thus avoiding any interferences with the steering wheel commands as shown in Fig. 5. The algorithm is robust enough when 3 or more markers are attached to the steering wheel. Moreover, if one marker is not well detected, its position is estimated processing its previous position and the current positions of other visible markers. Despite all these advantages, it is not exempt from defects: in presence of bright conditions or obstacles that totally obstructs the camera view, the algorithm may provide a wrong estimation of the steering wheel angle.

Sideslip angle estimation

Vehicle sideslip angle, together with yaw rate and lateral acceleration, provides a deep insight of vehicle lateral response to a driver-imposed steering wheel angle. It is defined as:

$$\beta = \arctan\left(\frac{v}{u}\right) \tag{3}$$

where u and v are respectively the longitudinal and lateral components of the vehicle speed measured at its center of gravity.

The sideslip angle provides an estimation on vehicle lateral drift, thus being a fundamental quantity for vehicle stability or “fun-to-drive”.

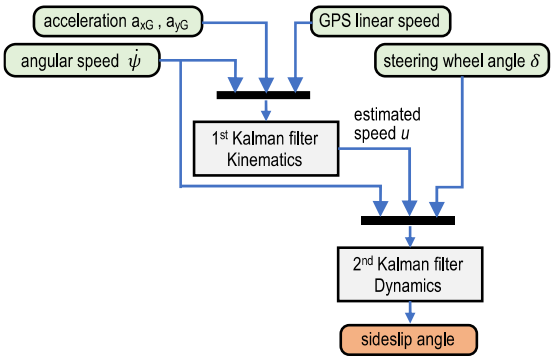

Figure 6. Cascade Kalman Filter scheme.

The smartphone does not have specific sensor for a direct measurement of vehicle sideslip angle, so two cascade Kalman Filters are implemented by adopting different vehicle models as highlighted in Fig. 6: a kinematic vehicle model is firstly adopted for estimating the vehicle longitudinal speed component starting from measured accelerations and the total vehicle speed obtained by the GPS; a single-track vehicle model is then considered for estimating the lateral component of vehicle speed thus calculating the sideslip angle from Eq. 3.

Kinematic vehicle model

This first model is one of the simplest vehicle models, since it relies on the kinematics relations between accelerations and angular speeds of a rigid body that can move on a horizontal plane:

$$\begin{pmatrix}\dot{u}\\ \dot{v}\end{pmatrix} = \underbrace{\begin{bmatrix}0 & \dot{\psi}\\ -\dot{\psi} & 0\end{bmatrix}}_{\boldsymbol{A}}\begin{pmatrix}u\\ v\end{pmatrix} + \underbrace{\begin{bmatrix}1 & 0\\ 0 & 1\end{bmatrix}}_{\boldsymbol{B}}\begin{pmatrix}a_{x_G}\\ a_{y_G}\end{pmatrix} \tag{4}$$

where $\dot{u}$ and $\dot{v}$ are the time derivative of longitudinal and lateral vehicle speed components respectively.

This model has the advantage of being independent on vehicle parameters, relying only on the smartphone measurements. The main drawback is that it requires the accelerations components of vehicle center of gravity as input of the model. These measurements are affected by noise and offset perturbations with respect to their actual values. Moreover, even if the accuracy of the smartphone accelerometers were extremely high and in total absence of noise and offset interference, the transformation of acceleration values on vehicle center of gravity depends on Eq. 2 and on the availability of $\ddot{\psi}$, $\ddot{\theta}$, $\ddot{\varphi}$, x_S, y_S and z_S. On the contrary, vehicle yaw rate $\dot{\psi}$ does not depend on the measurement point and it is more reliable than vehicle acceleration for estimation purposes.

The discretized version of Eq. 4 is obtained by considering the discrete derivative based on smartphone sampling time T_S:

$$\begin{pmatrix}u_{k+1}\\ v_{k+1}\end{pmatrix} = \underbrace{\begin{bmatrix}1 & T_S\dot{\psi}_k\\ -T_S\dot{\psi}_k & 1\end{bmatrix}}_{\boldsymbol{A}_k}\begin{pmatrix}u_k\\ v_k\end{pmatrix} + \underbrace{\begin{bmatrix}T_S & 0\\ 0 & T_S\end{bmatrix}}_{\boldsymbol{B}_k}\begin{pmatrix}a_{x_{G,k}}\\ a_{y_{G,k}}\end{pmatrix} \tag{5}$$

where the subscript k refers the kT_s time instant, $\boldsymbol{A}_k$ is the state matrix and $\boldsymbol{B}_k$ is the input matrix.

Single-track vehicle model

The kinematic model described in the previous section is adequate to provide a good estimation of vehicle longitudinal speed from to the one measured through smartphone GPS. A single-track model is then introduced for vehicle lateral speed estimation.

This second model relies on the following hypothesis:

- the vehicle is assumed as a rigid body in motion on a plane with mass m and mass moment of inertia J around Z_V-axis
- the front and rear axles are considered as an equivalent front and rear tires respectively
- the front steering angle δ_1 is applied as input by the driver
- vehicle speed is assumed constant
- two degrees of freedom: yaw rate and sideslip angle
- vehicle sideslip angle β and tires slip angles α_1 and α_2 are considered small enough to linearize the trigonometric functions
- curvature radius R much greater than vehicle wheelbase L

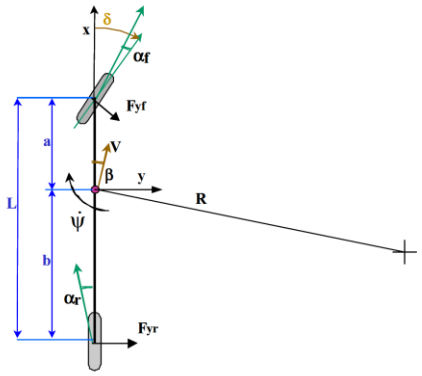

Figure 7. Single-track model scheme.

By referring to Fig. 7, the lateral and yaw equilibrium equations are expressed by:

$$\begin{cases} m(\dot{v} + u\dot{\psi}) = F_{yf} + F_{yr} \\ J\ddot{\psi} = F_{yf}a - F_{yr}b \end{cases} \quad (6)$$

where a and b are the front and the rear semi-wheelbase respectively and F_{yf}, F_{yr} are the front and rear axles lateral forces respectively, which can be expressed as linear functions of tires slip angles α_f and α_r:

$$\begin{aligned} F_{yf} &= C_f\alpha_f \\ F_{yr} &= C_r\alpha_r \end{aligned} \quad (7)$$

where C_f and C_r are the front and rear axles cornering stiffnesses.

To consider the change of the cornering stiffness with the lateral acceleration a parabolic relation is introduced:

$$C_{f/r} = C_{f/r\,0} - \left(\frac{a_y}{a_y|_{Cf/r=0}}\right)^2 C_{f/r\,0} \quad (8)$$

where $a_y|_{Cf/r=0}$ is the value of lateral acceleration correspondent to a null cornering stiffness, which must be set outside the working range of the car at least for one axle.

The model equations are finally correlated with the following kinematic relations:

$$\begin{aligned} \alpha_f &= \delta - \frac{v + \dot{\psi}\alpha_f}{u} = \tau\delta_{sw} - \frac{v + \dot{\psi}\alpha_f}{u} \\ \alpha_r &= -\frac{v - \dot{\psi}\alpha_r}{u} \end{aligned} \quad (9)$$

where τ is the steering ratio and δ_{sw} is the steering wheel angle.

Equations 6-9 can be finally grouped into the following matrix equation:

$$\begin{pmatrix} \dot{v} \\ \ddot{\psi} \end{pmatrix} = \begin{bmatrix} -\frac{C_f + C_r}{mu} & -\left(\frac{C_f a - C_r b}{mu} + u\right) \\ -\frac{C_f a - C_r b}{Ju} & -\frac{C_f a^2 + C_r b^2}{Ju} \end{bmatrix} \begin{pmatrix} v \\ \dot{\psi} \end{pmatrix} + \begin{bmatrix} \frac{C_f \tau}{m} \\ \frac{C_f a\, \tau}{J} \end{bmatrix} \delta_{sw} \quad (10)$$

where $\boldsymbol{x} = [v\ \dot{\psi}]'$ is the state vector and δ_{sw} is the input. The former equation can be rewritten in a more compact matrix form using the state-space representation:

$$\begin{cases} \dot{\boldsymbol{x}} = \boldsymbol{A(t)x} + \boldsymbol{Bw} \\ y = \boldsymbol{Cx} \end{cases} \quad (11)$$

where $\boldsymbol{w} = \delta_{sw}$ is the input vector, $y = \dot{\psi}$ the measurement output, ***A(t)*** the time-variant state matrix, ***B*** the input matrix, ***C*** the output matrix. It must be noted that the vehicle longitudinal speed u has a non-linear relation with respect to the model states, as can be seen in Eq. 10. Since the value of this quantity is known, thanks to GPS data, the state matrix ***A*** is not a constant matrix, but it is time variant due to the vehicle longitudinal dynamics and it should be therefore updated at each time step.

The discretized version of Eq. 10 is obtained by considering the discrete derivative based on smartphone sampling time T_S:

$$\begin{pmatrix} v_{k+1} \\ \dot{\psi}_{k+1} \end{pmatrix} = \underbrace{\begin{bmatrix} 1 - \frac{C_1 + C_2}{mu}T_S & -\left(\frac{C_1 a_1 - C_2 a_2}{mu} + u\right)T_S \\ -\frac{C_1 a_1 - C_2 a_2}{Ju}T_S & 1 - \frac{C_1 a_1^2 + C_2 a_2^2}{Ju}T_S \end{bmatrix}}_{\boldsymbol{A_k}} \begin{pmatrix} v_k \\ \dot{\psi}_k \end{pmatrix} + \underbrace{\begin{bmatrix} \frac{C_1 \tau}{m}T_S \\ \frac{C_1 a_1 \tau}{J}T_S \end{bmatrix}}_{\boldsymbol{B_k}} \delta_{v,k} \quad (12)$$

where the subscript k refers the kT_s time instant, $\boldsymbol{A}_k$ is the state matrix and $\boldsymbol{B}_k$ is the input matrix.

Kalman Filters Implementation

The Kalman Filter is a well-known algorithm that uses a series of measurements observed over time for estimating desired variables through a two-step process:

1. A time update phase that produces estimates of the current state variables through a mathematical model
2. A measurement update phase that corrects the former estimation using the available experimental data

Two covariance matrices are required for the Kalman Filter implementation:

- The process noise covariance $Q \in \mathbb{R}^{nxn}$, where n is the number of the mathematical model states.
- The measurement noise covariance $R \in \mathbb{R}^{mxm}$, where m is the number of measured states.

The algorithm is recursive, and it works also in real time by using only the current input measurements and the previously calculated state with its uncertainty matrix.

Two Kalman Filters are designed for the Smart Measuring System, as highlighted in Fig. 6: one for estimating the longitudinal vehicle speed through the kinematic model and a second one for estimating the sideslip angle through a single-track model.

The time update equations are responsible for projecting forward the current state (Eq.13) and error covariance (Eq.14) estimates to obtain the *a priori* or predicted estimates for the next time step:

$$\boldsymbol{x}_k^P = \boldsymbol{A}_k \boldsymbol{x}_{k-1} + \boldsymbol{B}_k \boldsymbol{w}_k \tag{13}$$

where $\boldsymbol{x}_k^P = [u_k \; v_k]'$ is the *a priori* or predicted state vector from the kinematic model and $\boldsymbol{x}_k^P = [v_k \; \dot{\psi}_k]'$ the one from the single track model; $\boldsymbol{w}_k = [a_{x_{G,k}} \; a_{y_{G,k}}]'$ is the input vector for the kinematic model and $\boldsymbol{w}_k = \delta_{v,k}$ is for the single-track model. Matrices $\boldsymbol{A}_k$ and $\boldsymbol{B}_k$ are defined in Eq. 5 and Eq. 12 for the kinematic and single-track models respectively.

The predicted covariance matrix is obtained by the following expression:

$$\boldsymbol{P}_k^P = \boldsymbol{A}_k \, \boldsymbol{P}_{k-1} \, \boldsymbol{A}_k^T + \boldsymbol{Q} \tag{14}$$

where $\boldsymbol{P}_k^P$ is the the *a priori* or predicted error covariance estimates and $\boldsymbol{P}_{k-1}$ is the error covariance estimated in the previous time step.

The measurement update equations are responsible for the feedback, i.e. for incorporating a new measurement into the *a priori* estimate to obtain an improved *a posteriori* estimate. The first task during the measurement update is to compute the Kalman gain K_k:

$$\boldsymbol{K}_k = \boldsymbol{P}_k^P \, \boldsymbol{C}^T \left(\boldsymbol{C} \boldsymbol{P}_k^P \boldsymbol{C}^T + \boldsymbol{R} \right)^{-1} \tag{15}$$

where $\boldsymbol{C}_k = [1 \; 0]$ is the output matrix for the kinematic model and $\boldsymbol{C}_k = [0 \; 1]$ for the single-track model.

The next step is to measure the process to obtain y_k, and then to generate a *posteriori* state $\hat{\boldsymbol{x}}_k$ (Eq. 16) and error covariance $\hat{\boldsymbol{P}}_k$ (Eq.17) estimates.

$$\hat{\boldsymbol{x}}_k = \boldsymbol{x}_k^P + \boldsymbol{K}_k \left(y_k - \boldsymbol{C} \, \boldsymbol{x}_k^P \right) \tag{16}$$

$$\hat{\boldsymbol{P}}_k = [\boldsymbol{I} - \boldsymbol{K}_k \boldsymbol{C}] \boldsymbol{P}_k^P \tag{17}$$

where $y_k = u_k$ is the measurement output for the kinematic model (from GPS data) and $y_k = \dot{\psi}_k$ for the single-track model.

Test track experimental validation

After a preliminary proof-of-concept phase, when an extensive validation of the process and algorithm was carried out adopting virtual analysis based on accurate vehicle simulators, the Smart Measuring System was tested on a real car driven on a test track for the final experimental validation.

The handling circuit of ASC (Automotive Safety Centre) in Vairano di Vidigulfo (Italy) was used to test the first prototypes into a real-world scenario. As can be observed in Fig. 8, it is a tortuous and very technical circuit having the following main features: length 2.6 km, width 7.5 m, maximum straight 350 m, maximum bend radius 400 m, minimum bend radius 12 m, clockwise driving direction.

A professional driver drove three cars belonging to different segments: a city car (B segment), a mid-size sport sedan and a pick-up. A typical measuring system used for vehicle handling analysis, already described in section “Data acquisition systems”, was installed on the car and used as reference for the assessment of the smart measuring system.

Figure 8. Top view of the handling test track. The red line is the car trajectory during a lap.

The smartphone was fixed to the driver's side window by means of a mobile phone holder with suction cup and it was oriented so that the rear camera can frame the steering wheel angle on which ArUco markers were attached, as shown in Fig. 9.

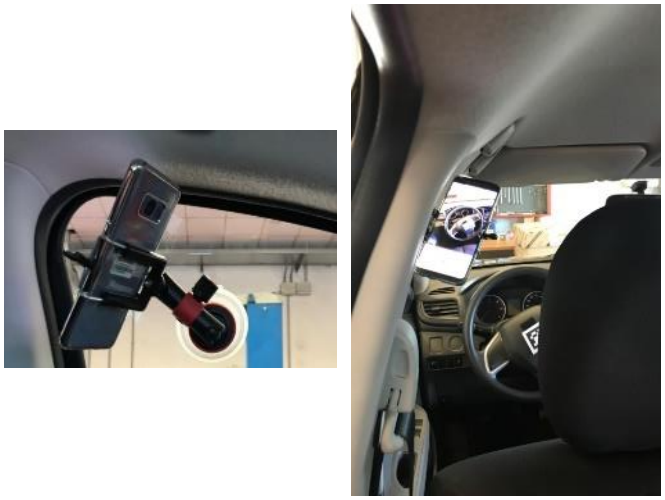

Figure 9. Typical smartphone installation on a car: mobile phone fixed to the driver's front window via a suction holder (left), smartphone position and orientation in the car cabin (right).

The typical handling quantities, that might be either directly measured or estimated, from the two systems working in parallel were collected and compared in post processing as explained in the following sections.

Direct measurements comparison

In this section, the comparison between Smart Measuring System and professional measurements in terms of accelerations, angular speeds and steering wheel angle during the initialization phase and a single lap on the handling test track are shown.

First, the initialization phase is analyzed. The most interesting signal in this case is vehicle longitudinal acceleration. In Fig. 10 the signals from the smart measuring system, named APP in the figures, and the professional system, named VBOX, are compared in time domain. At second 2, vibration due to engine start is clearly visible from the time history, at second 8.5 the car is accelerated in first gear and then braked starting from second 13, a similar sequence of acceleration and braking is repeated from second 18 to 30. The two signals overlap very well both allowing to distinguish the aforementioned phases and the frequency content of each of them. The unfiltered APP data appear noisier due to vibration induced by the mobile phone holder compliance.

The natural frequency of the supporting system, which was identified to be 15.5 Hz, is well above the frequency range of handling analysis, i.e. 0-3 Hz; hence it does not interfere with the measure of chassis rigid body dynamics. More specifically, the spectrograms of the three components of chassis acceleration were analyzed with the aim of identifying the natural frequency of the supporting system. In Fig. 11, as an example, the spectrogram of the vertical acceleration measured during an initialization phase is reported and the resonance frequency located.

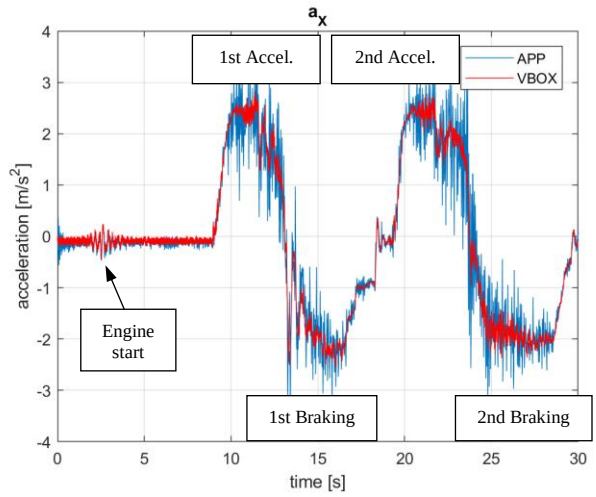

Figure 10 – Longitudinal acceleration during the initialization phase.

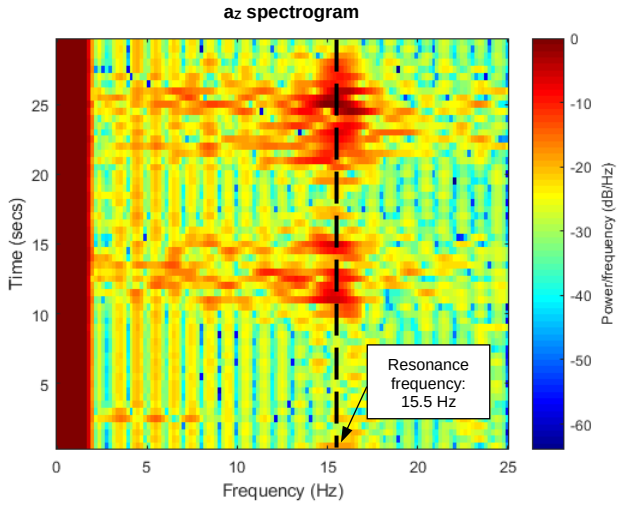

Figure 11 – Spectrogram of the vertical acceleration and identification of the natural frequency of the supporting system during the initialization phase. The reference value for dB is 1 m/s^2.

The experimental validation of the smart measuring system was then carried out by comparing the time histories of signals relevant for handling analysis. Data from VBOX system were used as reference to validate the measures/estimates from APP. Fig. 12 and Fig.13 plot the trends of longitudinal and lateral components of the vehicle acceleration. Although the APP data are noisier, as already explained for the initialization phase, the main dynamics of the signals are properly captured. Fig. 14 and Fig.15 show the trends of steering wheel angle and yaw rate.

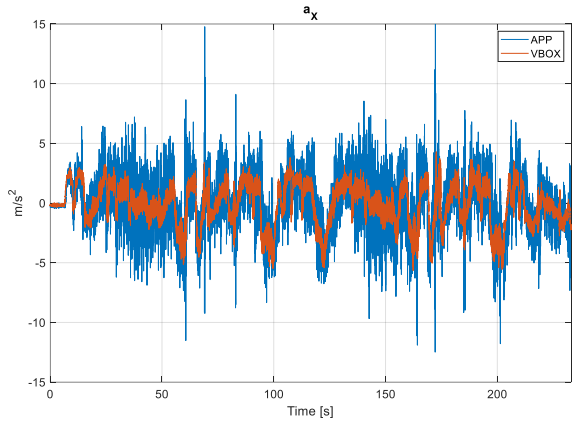

Figure 12 – Experimental validation: longitudinal acceleration during a lap on the handling test track.

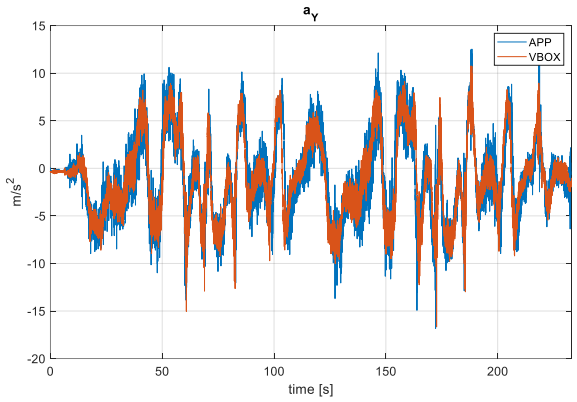

Figure 13 – Experimental validation: lateral acceleration during a lap on the handling test track.

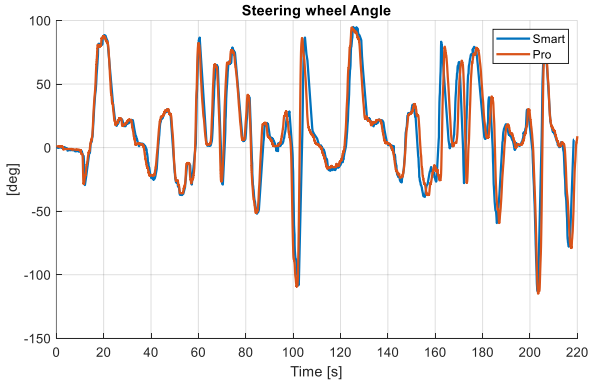

Figure 14 – Experimental validation: steering wheel angle during a lap on the handling test track.

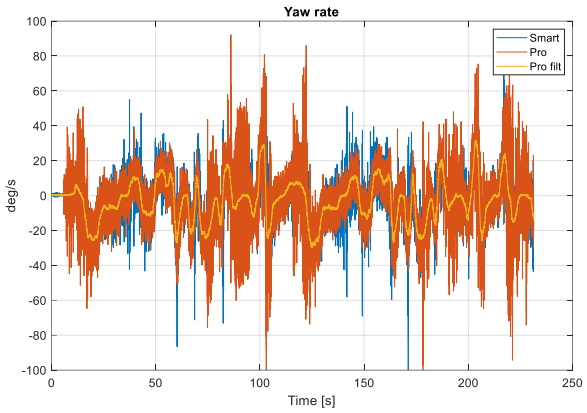

Figure 15 – Experimental validation: yaw rate during a lap on the handling test track.

By applying a 2nd order Butterworth type low pass filter with cut-off frequency set at 13 Hz to the raw data from smart system, trends like the one shown in Fig. 16, where the filtered yaw rate signals are compared, can be obtained.

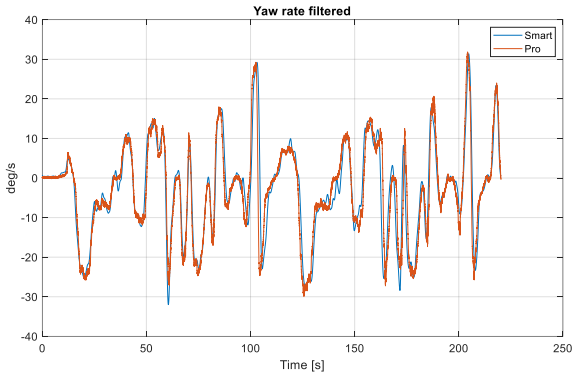

Figure 16 – Experimental validation: filtered yaw rate.

The comparison of the measures from the two systems, shown in Figures 12-16, highlights a very good correlation. The smart measurement is able to capture the dynamics of interest for vehicle handling analysis. However, a variable phase lag is visible, e.g. at around 100 s in the figures, due to the lack of a shared clock system for all the smartphone sensors. The smart measuring system will be updated in the next App release to solve this synchronization issue.

Estimated sideslip angle comparison

In this section, results from the sideslip angle estimation algorithm based on Kalman filters are compared with the measures made by the dual antenna GPS system.
Before the test, the cars used on the proving ground were weighted in their final setup, considering driver, passengers and equipment. The longitudinal position of the center of gravity was then estimated knowing the axles weight. The values of wheelbase and steering ratio were available from cars data sheets.
The cornering stiffnesses of front and rear axle have been optimized so that the estimation error was minimum. The starting values and the variability range of these parameters are typical of the considered car segment. The idea, for non-professional users of the smart system, is

to allow them selecting simply the car segment from a list and then load a set of values for the bicycle model parameters which are representative of the selected car type, that will be used for the dynamic Kalman filter initialization.
Two cars belonging to different segments were considered for the assessment of the smart measuring system, a fastback coupé (Vehicle A) and a pick-up truck (Vehicle B). The single-track model parameters for these two vehicles are reported in Table 1.
The covariance matrices were tuned and then they are kept the same for both cars. The only difference between the two estimators are the values of the two car models.

Table 1. Parameters of the two vehicles used in the Kalman sideslip estimator.

	Vehicle A	**Vehicle B**
Type	Fastback Coupé	Pick-up Truck
a [mm]	1190	1336
b [mm]	1380	1664
m [kg]	1446	2226
J [kg m^2]	1800	2500
τ [-]	1/12.5	1/17
C_{f0} [kN/rad]	130	150
C_{r0} [kN/rad]	110	145
$a_y\|_{Cf,Cr=0}$ [g]	1.12	1.02
$rms(\beta_{Pro} - \beta_{smart})$ [°]	0.56	0.55
Q_0	diag([0.005 0.005])	
R_0	0.1	

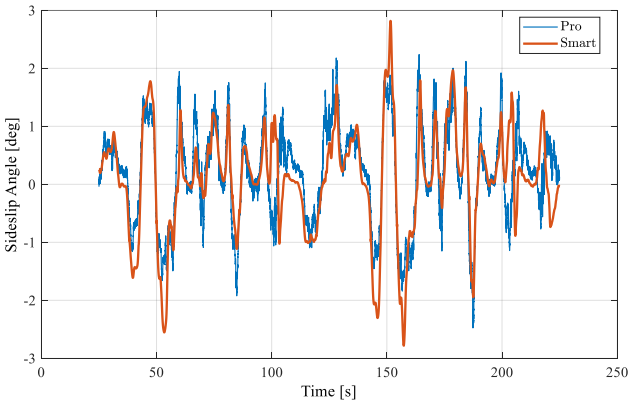

Figure 16 – Side-slip angle during a fast lap on the handling test track: comparison between measure by dual antenna (Pro) and estimation based on Kalman filter (Smart). Vehicle A.

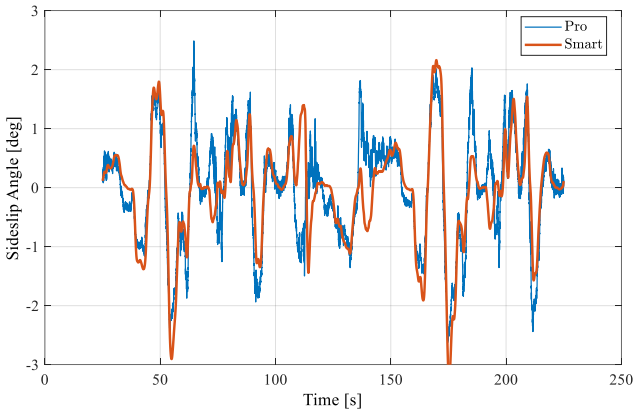

Figure 17 – Side-slip angle during a fast lap on the handling test track: comparison between measure by dual antenna (Pro) and estimation based on Kalman filter (Smart). Vehicle B.

Fig. 16 and Fig. 17 show the sideslip angle time histories during the fast lap on the handling circuit travelled by the two selected vehicles. The Kalman filter side slip angle estimator based on single-track model with variable cornering stiffness proved to be suitable to perform the task even in these extreme dynamic conditions. The rms of the error during the reported tests is less than 0.6 degrees for both cars, that is an acceptable value for the aim of this instrumentation.
If the mean value of the cornering stiffness is used (i.e. 70% of the maximum value C_0 reported in the Table) instead of implementing their dependency on lateral acceleration, the error increases by 20% for Vehicle B, and by 3% for Vehicle A.

In the absence of a professional measuring system that can be used as a reference for the filter tuning, a robust identification procedure is needed to find the right cornering stiffness values and more in general the lacking model parameter values. For instance, a steady-state cornering maneuver like steering pad and a transient maneuver like sweep steer are suitable tests allowing parameter identification.

Conclusions

In this paper a novel measuring system based on the sensors available on a smartphone aiming at fast vehicle handling evaluation has been presented. The remarks of the activity are:

- a preliminary vibration analysis of the mobile phone supporting system showed that its natural frequency is well above the maximum frequency considered in handling analysis, so it does not significantly interfere with the quality of the measure;
- although the APP data are noisier, due to the compliance of the supporting system, the main dynamics of the signals are properly captured;
- a simple low-pass filter is effective to extract the trend of the signals of interest from raw data coming from sensors;
- the sensors available in a top-class smartphone are accurate and with a bandwidth compliant with typical handling analysis requirements;
- the Kalman filter estimator proved an effective method for side slip angle estimation but requires model parameters values;
- an automatic tuning procedure will be developed in the future to automatically detect the model parameters by using

steady-state cornering events, especially for cornering stiffness identification, and transient events like sweep-steer;
- the system can be effectively used for a fast and cheap evaluation of the vehicle dynamics for private and professional usage.

Acknoledgments

The authors wish to thank Politecnico di Torino for its financial support within the Proof of Concept project (PoC).

References

1. Velardocchia, M., Vigliani, A. “Control systems integration for enhanced vehicle dynamics”, Open Mechanical Engineering Journal, 7(1) (2013): 58-69.
2. Morgando, A., Velardocchia, M., Vigliani, A., Van Leeuwen, B.G., Ondrak, V., “An alternative approach to automotive ESC based on measured wheel forces”, Vehicle System Dynamics, 49(12) (2011): 1855-1871.
3. Segers, Jorge. Analysis techniques for racecar data acquisition. Vol. 367. SAE Technical Paper, 2008.
4. Andria, G., et al. "Development of an automotive data acquisition platform for analysis of driving behavior." Measurement 93 (2016): 278-287.
5. https://www.kistler.com/en/product/type-cs350a/, available on 18/11/2019
6. https://www.navtechgps.com/oxts_xnav200/, available on 18/11/2019
7. Arndt, Dietmar. "Method and device for determining the float angle of a motor vehicle." U.S. Patent No. 7,058,486. 6 Jun. 2006.
8. Tin Leung, King, et al. "A review of ground vehicle dynamic state estimations utilising GPS/INS." Vehicle System Dynamics 49.1-2 (2011): 29-58.
9. Wang, Haoan, Tota, Antonio, Aksun-Guvenc, Bilin, & Guvenc, Levent. "Real time implementation of socially acceptable collision avoidance of a low speed autonomous shuttle using the elastic band method." Mechatronics 50 (2018): 341-355.
10. Tota, Antonio, Mauro Velardocchia, and Levent Güvenç. "Path Tracking Control for Autonomous Driving Applications." International Conference on Robotics in Alpe-Adria Danube Region. Springer, Cham, 2017.
11. Sharifzadeh, M., et al. "Real Time Tyre Forces Estimation for Advanced Vehicle Control." International Journal of Mechanics and Control, 18 (2017):77-84
12. Chindamo, Daniel, Basilio Lenzo, and Marco Gadola. "On the vehicle sideslip angle estimation: a literature review of methods, models, and innovations." Applied Sciences 8.3 (2018): 355.
13. Selmanaj, Donald, et al. "Robust vehicle sideslip estimation based on kinematic considerations." IFAC-PapersOnLine 50.1 (2017): 14855-14860.
14. Selmanaj, Donald, et al. "Vehicle sideslip estimation: A kinematic based approach." Control Engineering Practice 67 (2017): 1-12.
15. Lu, Qian, et al. "Enhancing vehicle cornering limit through sideslip and yaw rate control." Mechanical systems and signal processing 75 (2016): 455-472.
16. Cheli, Federico, et al. "A methodology for vehicle sideslip angle identification: comparison with experimental data." Vehicle System Dynamics 45.6 (2007): 549-563.
17. Dakhlallah, Jamil, Sebastien Glaser, and Said Mammar. "Vehicle side slip angle estimation with stiffness adaptation." International Journal of Vehicle Autonomous Systems 8.1 (2010): 56-79.
18. Piyabongkarn, Damrongrit, et al. "Development and experimental evaluation of a slip angle estimator for vehicle stability control." IEEE Transactions on control systems technology 17.1 (2008): 78-88.
19. Li, Xu, Xiang Song, and Chingyao Chan. "Reliable vehicle sideslip angle fusion estimation using low-cost sensors." Measurement 51 (2014): 241-258.
20. Leung, King Tin, et al. "Road vehicle state estimation using low-cost GPS/INS." Mechanical Systems and Signal Processing 25.6 (2011): 1988-2004.
21. Svensson, Johan. "Design of a portable steering wheel angle measurement system." (2015).
22. Hoeller, Reinhold, et al. "Combined steering angle and torque sensor." U.S. Patent No. 7,726,208. 1 Jun. 2010.
23. Chowdhury, Mazharul, et al. "Non-contact angle/torque sensor for steering apparatus of vehicle." U.S. Patent No. 10,234,263. 19 Mar. 2019.

Contact Information

enrico.galvagno@polito.it